Chemistry and Physics of Lipids 201 (2016) 41–49

Contents lists available at ScienceDirect

Chemistry and Physics of Lipids

journal homepage: www.elsevier.com/locate/chemphyslip

Effect of local anesthetics on serotonin$_{1A}$ receptor function

Bhagyashree D. Rao[a,c], Sandeep Shrivastava[b], Amitabha Chattopadhyay[b,c,*]

[a] CSIR-Indian Institute of Chemical Technology, Uppal Road, Hyderabad 500 007, India
[b] CSIR-Centre for Cellular and Molecular Biology, Uppal Road, Hyderabad 500 007, India
[c] Academy of Scientific and Innovative Research, New Delhi, India

ARTICLE INFO

Article history:
Received 14 September 2016
Received in revised form 27 October 2016
Accepted 1 November 2016
Available online 5 November 2016

Keywords:
Phenylethanol
Local anesthetics
Hippocampal membranes
Membrane order
G-protein coupling
Serotonin$_{1A}$ receptor

ABSTRACT

The fundamental mechanism behind the action of local anesthetics is still not clearly understood. Phenylethanol (PEtOH) is a constituent of essential oils with a pleasant odor and can act as a local anesthetic. In this work, we have explored the effect of PEtOH on the function of the hippocampal serotonin$_{1A}$ receptor, a representative neurotransmitter receptor belonging to the G protein-coupled receptor (GPCR) family. Our results show that PEtOH induces reduction in ligand binding to the serotonin$_{1A}$ receptor due to lowering of binding affinity, along with a concomitant decrease in the degree of G-protein coupling. Analysis of membrane order using the environment-sensitive fluorescent probe DPH revealed decrease in membrane order with increasing PEtOH concentration, as evident from reduction in rotational correlation time of the probe. Analysis of results obtained shows that the action of local anesthetics could be attributed to the combined effects of specific interaction of the receptor with anesthetics and alteration of membrane properties (such as membrane order). These results assume relevance in the perspective of anesthetic action and could be helpful to achieve a better understanding of the possible role of anesthetics in the function of membrane receptors.

1. Introduction

Local anesthetics belong to a group of amphiphilic compounds which curb the feeling of pain, when applied in a particular part of the body by preventing the transmission of nerve impulse, thereby reducing the pain in that area. In spite of a large body of work, the molecular mechanism by which local anesthetics act is not understood. Two predominant models have been suggested to explain anesthetic action. The first model, the lipid hypothesis, attributes the anesthetic effect to variations in membrane physical properties. According to this model, changes in the physical (global) properties of the membrane (*e.g.*, membrane order) modulate membrane protein function (Rehberg et al., 1995). The second model, known as the protein hypothesis, attributes anesthetic effect to specific interaction of anesthetics with membrane proteins, thereby affecting membrane protein function (Arias, 1999). It is still not clear whether anesthetic action is an outcome of indirect anesthetic-lipid effect or a more direct anesthetic-protein interaction. Yet another way to understand the basis of anesthetic effects is to explore changes in the lateral pressure profiles in membrane bilayers due to addition of anesthetics (Cantor, 2001). In this overall scenario, a useful approach for understanding the molecular mechanism of local anesthetics is to identify specific targets of anesthetics.

Phenylethanol (PEtOH) (see inset of Fig. 1) is found in a variety of essential oils, it has a fragrant rose-like odor, and can act as a local anesthetic (Anbazhagan et al., 2010; Gray et al., 2013). It also possesses antibacterial activity (Corre et al., 1990). Interestingly, PEtOH has been reported to vary membrane order by altering the packing of lipid molecules (Anbazhagan et al., 2010; Jordi et al., 1990; Killian et al., 1992). We have recently shown that PEtOH causes disorder in various membrane phases (gel, fluid and liquid-ordered), although the disorder was found to be phase-specific (Shrivastava et al., 2016). Moreover, PEtOH has been shown to bring about translocation of the mitochondrial precursor protein apocytochrome *c* (Jordi et al., 1990), and modulate oligomerization of membrane proteins in *E. coli* by perturbing helix-helix interaction (Anbazhagan et al., 2010).

Abbreviations: 8-OH-DPAT, 8-hydroxy-2(di-*N*-propylamino)tetralin; BCA, bicinchoninic acid; DMPC, 1,2-dimyristoyl-*sn*-glycero-3-phosphocholine; DPH, 1,6-diphenyl-1,3,5-hexatriene; GPCR, G protein-coupled receptor; GTP-γ-S, guanosine-5′-*O*-(3-thiotriphosphate); PEtOH, phenylethanol; *p*-MPPF, 4-(2′-methoxy)-phenyl-1-[2′-(*N*-2″-pyridinyl)-*p*-fluorobenzamido]ethyl-piperazine; PMSF, phenylmethylsulfonyl fluoride.

* Corresponding author at: CSIR-Centre for Cellular and Molecular Biology, Uppal Road, Hyderabad 500 007, India. Tel.: +91 40 2719 2578; fax: +91 40 2716 0311.
E-mail address: amit@ccmb.res.in (A. Chattopadhyay).

http://dx.doi.org/10.1016/j.chemphyslip.2016.11.001
0009-3084/

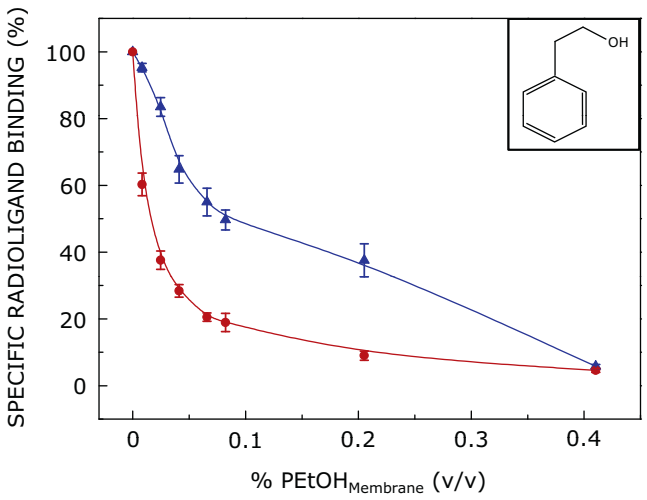

Fig. 1. Specific binding of the agonist [^{3}H]8-OH-DPAT (●), and the antagonist [^{3}H]*p*-MPPF (▲) to the serotonin$_{1A}$ receptor with increasing concentrations of the local anesthetic, PEtOH. The PEtOH concentration plotted here is the actual concentration of PEtOH partitioned into the membrane (see Table 1). Values are expressed as a percentage of the specific ligand binding obtained in the absence of PEtOH. Data points represent means ± S.E. of duplicate points from at least three independent experiments. The line joining the data points is provided merely as a viewing guide. The inset shows the chemical structure of PEtOH. See Section 2 for more details.

G protein-coupled receptors (GPCRs), which characteristically possess seven transmembrane domains, form the largest superfamily of membrane proteins implicated in information transfer from the extracellular region to the interior of cells (Chattopadhyay, 2014; Pierce et al., 2002; Rosenbaum et al., 2009). The total number of GPCRs is close to 800 belonging to different families (Fredriksson et al., 2003), and ∼5% of human genes encode them (Zhang et al., 2006). GPCRs play a central role in mediating diverse physiological processes and a wide array of ligands including light are responsible for their activation. As GPCRs are implicated in multiple physiological responses, they represent popular targets for currently prescribed drugs in all clinical areas and are useful for the development of novel drugs (Jacobson, 2015; Tautermann, 2014). Yet, new functions associated with GPCRs are still being explored. Serotonin receptors are an important class of GPCRs which bind the neurotransmitter serotonin (Nichols and Nichols, 2008). The serotonin$_{1A}$ receptor occupies a unique position among members of the serotonin receptor family for a number of reasons (Pucadyil et al., 2005). The serotonin$_{1A}$ receptor has emerged as a crucial target in developing new drugs to treat a range of diseases from anxiety and depression to cancer (Fiorino et al., 2014).

Among membrane proteins, ion channels appear to be the most common targets of anesthetic action (Arias, 1999; Fozzard et al., 2005; Franks and Lieb, 1997). On the other hand, involvement of GPCRs in anesthetics action is an emerging area. Although there are some reports on the interaction of GPCRs with anesthetics (Hollmann et al., 2005; Ishizawa et al., 2002; Kalipatnapu and Chattopadhyay, 2004; Matsunaga et al., 2015; Nakayama et al., 2005; Peterlin et al., 2005; Picardi et al., 2014), detailed information on interaction of GPCRs with local anesthetics with respect to affinity of binding and influence on membrane order, and their relative importance in anesthetic action, is lacking. Keeping this in mind, we have probed the effect of the local anesthetic PEtOH on serotonin$_{1A}$ receptor function. Our results show that PEtOH induces a decrease in specific ligand binding activity and G-protein coupling efficiency of the hippocampal serotonin$_{1A}$ receptor. There is a concomitant decrease in membrane order in presence of PEtOH. Our results show that both specific interaction of the receptor with anesthetics as well as alteration of global properties (such as membrane order) of the lipid environment could be involved in local anesthetic action.

2. Materials and methods

2.1. Materials

1,2-dimyristoyl-*sn*-glycero-3-phosphocholine (DMPC), EDTA, EGTA, $MgCl_2$, $MnCl_2$, Na_2HPO_4, iodoacetamide, PEtOH, 4-(2′-methoxy)-phenyl-1-[2′-(*N*-2″-pyridinyl)-*p*-fluorobenzamido]ethyl-piperazine dihydrochloride (*p*-MPPF), PMSF, polyethylenimine, serotonin hydrochloride, sodium azide, sucrose and Tris were purchased from Sigma Chemical Co. (St. Louis, MO). [^{3}H]8-hydroxy-2(di-*N*-propylamino)tetralin ([^{3}H]8-OH-DPAT) (specific activity 187.4 Ci/mmol) and [^{3}H]*p*-MPPF (specific activity 74.2 Ci/mmol) were purchased from MP Biomedicals (Santa Ana, CA). Bicinchoninic acid (BCA) assay reagent for protein estimation was from Pierce (Rockford, IL). GF/B glass microfiber filters were from Whatman International (Kent, UK). GTP-γ-S (guanosine-5′-*O*-(3-thiotriphosphate)) was purchased from Roche Applied Science (Mannheim, Germany). DPH was purchased from Molecular Probes/Invitrogen (Eugene, OR). The concentration of a stock solution of DPH prepared in methanol was calculated using its molar extinction coefficient (ε) of 88,000 M^{-1} cm^{-1} at 350 nm in methanol. All other chemicals used were of the highest purity available. Solvents used were of spectroscopic grade. Water was purified through a Millipore (Bedford, MA) Milli-Q system and used throughout. Stock solution of PEtOH (2% (v/v)) was prepared in 50 mM Tris buffer (pH 7.4) and used for experiments. Fresh bovine brains were procured from a local slaughterhouse within 10 min of death, and the hippocampal region was cautiously cut out. The hippocampi were immediately flash frozen in liquid nitrogen and stored at −80 °C till further use.

2.2. Methods

2.2.1. Preparation of native hippocampal membranes

Native hippocampal membranes were prepared as described previously (Pucadyil and Chattopadhyay, 2004a). Briefly, hippocampal tissue (∼50 g) was homogenized as 10% (w/v) in a polytron homogenizer in 2.5 mM Tris, 0.32 M sucrose, 5 mM EDTA, 5 mM EGTA, 0.02% sodium azide, 0.24 mM PMSF, 10 mM iodoacetamide, pH 7.4 buffer. The homogenate was centrifuged at 900 × *g* for 10 min at 4 °C. The resultant supernatant was filtered through three layers of cheesecloth and centrifuged at 50,000 × *g* for 20 min at 4 °C. The pellet obtained was suspended in 10 vol. of 50 mM Tris, 1 mM EDTA, 0.24 mM PMSF, 10 mM iodoacetamide, pH 7.4 buffer using a hand-held Dounce homogenizer and centrifuged at 50,000 × *g* for 20 min at 4 °C. This procedure was repeated until a clear supernatant was obtained. The final pellet was suspended in a minimum volume of 50 mM Tris (pH 7.4) buffer, homogenized using a hand-held Dounce homogenizer, flash frozen in liquid nitrogen and stored at −80 °C. Protein concentration was assayed using BCA reagent with bovine serum albumin as standard (Smith et al., 1985).

2.2.2. Radioligand binding assays

Receptor binding assays were conducted as described previously (Harikumar and Chattopadhyay, 1999; Pucadyil and Chattopadhyay, 2004a). Briefly, tubes in duplicate with ∼1 mg protein in a total volume of 1 ml of buffer (50 mM Tris, 1 mM EDTA, 10 mM $MgCl_2$, 5 mM $MnCl_2$, pH 7.4) were incubated with the radiolabeled agonist [^{3}H]8-OH-DPAT for 1 h at room temperature (25 °C). For antagonist binding with [^{3}H]-*p*-MPPF, the buffer did not contain $MgCl_2$ and $MnCl_2$. The final concentrations of both agonist and

antagonist in each assay tube was 0.5 nM. Nonspecific binding was determined by conducting the assay in the presence of 10 μM serotonin (for agonist binding) or *p*-MPPF (for antagonist binding). The binding reaction was terminated by rapid filtration under vacuum in a Millipore multiport filtration apparatus through Whatman GF/B 2.5 cm diameter glass microfiber filters (1.0 μm pore size) which were presoaked in 0.3% polyethylenimine for 1 h (Bruns et al., 1983). Filters were washed three times with 3 ml of cold water (4 °C), dried and the retained radioactivity was measured in a Packard Tri-Carb 2900 liquid scintillation counter using ~5 ml of scintillation fluid.

2.2.3. Saturation binding assays

Saturation binding assays were performed with increasing concentrations (0.1–12.5 nM) of the radiolabeled agonist [^{3}H]8-OH-DPAT as described previously (Pucadyil and Chattopadhyay, 2004a), in presence of 0.04% (v/v) PEtOH. Binding assays were performed at room temperature (25 °C). The concentration of the bound ligand (RL*) was calculated from:

$$RL^* = 10^{-9} \times B/(V \times SA \times 2220)\ M \quad (1)$$

where B is the bound radioactivity in disintegrations per minute (dpm), V is the assay volume in ml, and SA is the specific activity of the radioligand. The data could be fitted best to a one-site ligand binding equation. The dissociation constant (K_d) and the number of maximum binding sites (B_{max}) were calculated by nonlinear regression analysis of binding data using Graphpad Prism software, version 4.0. Data obtained after regression analysis were used to plot graphs with Microcal Origin software, version 6.0 (OriginLab, Northampton, MA). The binding parameters were obtained by averaging the results of three independent experiments, while the saturation binding data shown in Fig. 2 is from a representative experiment.

2.2.4. GTP-γ-S sensitivity assay

To estimate the efficiency of G-protein coupling to the receptor in presence of PEtOH, GTP-γ-S sensitivity assays were carried out as described previously (Pucadyil and Chattopadhyay, 2004a). The concentration of PEtOH was 0.04% (v/v) and experiments were performed at room temperature (25 °C). The concentrations of GTP-γ-S leading to 50% inhibition of specific agonist binding (IC_{50}) were calculated by nonlinear regression fitting of the data to a four-parameter logistic function (Higashijima et al., 1987):

$$B = a[1 + (x/I)^s]^{-1} + b \quad (2)$$

where B is the specific binding of the agonist normalized to agonist binding at the lowest concentration of GTP-γ-S, x denotes the concentration of GTP-γ-S, a is the range (y_{max}–y_{min}) of the fitted curve on the ordinate (y-*axis*), I is the IC_{50} concentration, b is the background of the fitted curve (y_{min}), and s is the slope factor. IC_{50} values obtained and the GTP-γ-S sensitivity assay data shown in Fig. 3 were obtained by averaging the results of three independent experiments.

2.2.5. Estimation of inorganic phosphate

The concentration of lipid phosphate was determined subsequent to total digestion by perchloric acid (McClare, 1971) using Na_2HPO_4 as standard. DMPC was used as an internal standard to assess lipid digestion. Samples without perchloric acid digestion produced negligible readings.

2.2.6. Fluorescence anisotropy measurements

Fluorescence anisotropy measurements were performed with a Hitachi F-7000 spectrofluorometer (Tokyo, Japan) using Hitachi Glan-Thompson polarization accessory, as described previously (Shrivastava et al., 2016). The excitation wavelength was set at 358 nm and emission was monitored at 430 nm. Excitation and emission slits with bandpass of 2.5 and 10 nm were used for all measurements. The excitation slit was kept less to reduce any photoisomerization of DPH. Fluorescence was measured with a 30 s interval between consecutive openings of the excitation shutter to undo any photoisomerization of DPH (Chattopadhyay and London, 1984). The samples optical density measured at 358 nm was always less than 0.15. Anisotropy values were calculated from the equation (Lakowicz, 2006):

$$r = \frac{I_{VV} - GI_{VH}}{I_{VV} + 2GI_{VH}} \quad (3)$$

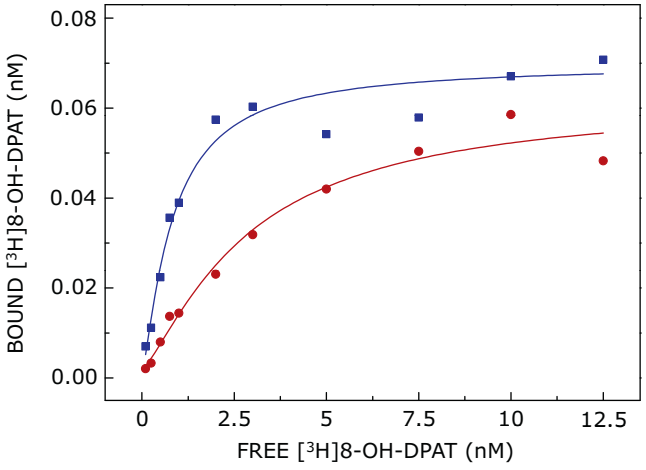

Fig. 2. Saturation binding analysis of specific [^{3}H]8-OH-DPAT binding to the serotonin$_{1A}$ receptor in hippocampal membranes in the presence of PEtOH. The concentration of [^{3}H]8-OH-DPAT ranged from 0.1 to 12.5 nM whereas PEtOH concentration used was 0.05% (v/v). Representative binding plots are shown for native (■) and PEtOH-treated (●) membranes. The curves are nonlinear regression fits to the experimental data. See Section 2 and Table 2 for more details.

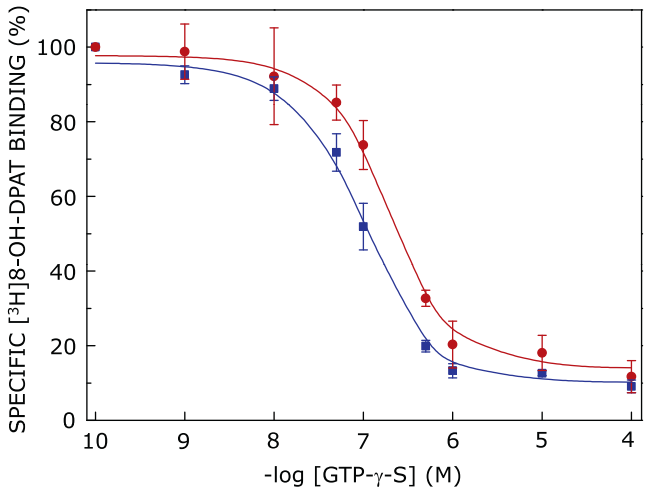

Fig. 3. Effect of increasing concentrations of GTP-γ-S on the specific binding of [^{3}H]8-OH-DPAT to the serotonin$_{1A}$ receptor in native (■) and PEtOH-treated (●) hippocampal membranes. The concentration of PEtOH used was 0.05% (v/v). Values are expressed as percentages of specific binding obtained in the presence of lowest concentration of GTP-γ-S. The curves are nonlinear regression fits to the experimental data. Data points shown are means ± S.E. of duplicate points from three independent experiments. The respective half maximal inhibition concentrations (IC_{50}) of GTP-γ-S, reflecting the efficiency of G-protein coupling to the receptor, are shown in Table 3. See Section 2 and Table 3 for more details.

where I_{VV} and I_{VH} are the fluorescence intensities (after background subtraction) measured with the excitation polarizer oriented vertically and the emission polarizer vertically and horizontally oriented, respectively. G is the grating factor and is the ratio of the efficiencies of the detection system for vertically and horizontally polarized light, and is equal to I_{HV}/I_{HH}. All experiments were performed at room temperature (25 °C) with at least three sets of samples and mean values of fluorescence anisotropy are shown in Fig. 4.

2.2.7. Time-resolved fluorescence measurements

Fluorescence lifetimes were calculated from time-resolved fluorescence intensity decays using IBH 5000F NanoLED equipment (Horiba Jobin Yvon, Edison, NJ) with DataStation software in the time-correlated single photon counting (TCSPC) mode, as described previously (Shrivastava et al., 2016), except that a pulsed light-emitting diode (LED) (NanoLED-370) was used as an excitation source. This LED generates optical pulse at 374 nm with pulse duration 1.2 ns and is run at 1 MHz repetition rate. All experiments were performed at room temperature (25 °C). Fluorescence intensity decay curves so obtained were deconvoluted with the instrument response function and analyzed as a sum of exponential terms:

$$F(t) = \Sigma_i\, \alpha_i \exp(-t/\tau_i) \quad (4)$$

where F(t) is the fluorescence intensity at time t and α_i is a pre-exponential factor representing the fractional contribution to the time-resolved decay of the component with a lifetime of τ_i such that $\Sigma_i \alpha_i = 1$. The goodness of the fit of a given set of observed data and the chosen function was evaluated by the χ^2 ratio, the weighted residuals (Lampert et al., 1983), and the autocorrelation function of the weighted residuals (Grinvald and Steinberg, 1974). A fit was considered good enough when plots of the weighted residuals and the autocorrelation function displayed random deviation about zero with a maximum χ^2 value of not more than 1.5. Intensity-averaged mean lifetimes $<\tau>$ for biexponential decays of fluorescence were calculated from the decay times and pre-exponential factors using the equation (Lakowicz, 2006):

$$\left\langle \tau \right\rangle = \frac{\alpha_1 {\tau_1}^2 + \alpha_2 {\tau_2}^2}{\alpha_1 \tau_1 + \alpha_2 \tau_2} \quad (5)$$

2.2.8. Statistical analysis

Student's two-tailed unpaired *t*-test was performed to estimate significance levels using Graphpad Prism software, version 4.0 (San Diego, CA). The correlation between specific agonist binding of the serotonin$_{1A}$ receptor with apparent rotational correlation time was analyzed with 90% confidence interval. Plots were generated using Microcal Origin software, version 6.0 (OriginLab, Northampton, MA).

3. Results

3.1. Actual concentration of PEtOH partitioned into the membrane

Previous results from mutagenesis (Ho et al., 1992; Chanda et al., 1993) and molecular modeling (Paila et al., 2011) studies have shown that in case of the serotonin$_{1A}$ receptor, the ligand binding site is localized in the transmembrane region. It is therefore crucial to know the actual concentration of PEtOH partitioned into hippocampal membrane with respect to effect of PEtOH on ligand binding to the serotonin$_{1A}$ receptor. Actual concentrations of PEtOH partitioning into the membrane were calculated using the membrane/buffer partition coefficient of PEtOH. The membrane/buffer partition coeffiecient of PEtOH is defined as:

$$P = C_M/C_B \quad (6)$$

where C_M and C_B represent the concentrations of PEtOH in membrane and buffer, respectively. The total (bulk) concentration of PEtOH is given by:

$$C_T = C_M + C_B \quad (7)$$

Substituting for C_B ($C_B = C_T - C_M$) from Eq. (7) into Eq. (6), we obtain:

$$P = C_M/(C_T - C_M) \quad (8)$$

Upon rearrangement of Eq. (8), we obtain:

$$C_M = PC_T/(1 + P) \quad (9)$$

Using the value of partition coefficient (4.58) of PEtOH from literature (McCreery and Hunt, 1978), the actual concentration of PEtOH partitioned in the membrane therefore can be calculated (see Table 1). The concentration of PEtOH plotted in Figs. 1, 4 and 5 are actual membrane concentrations determined this way, as shown in Table 1.

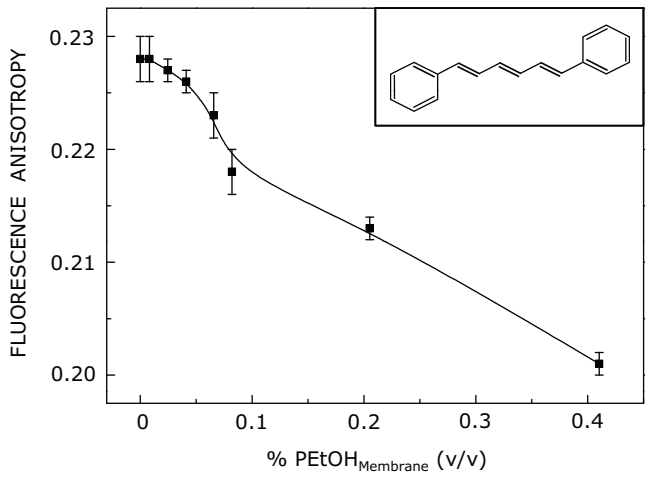

Fig. 4. Effect of PEtOH on fluorescence anisotropy of DPH in hippocampal membranes. Change in membrane order was calculated by measuring fluorescence anisotropy of DPH with increasing concentrations of PEtOH. The PEtOH concentration plotted here is the actual concentration of PEtOH partitioned into the membrane (see Table 1). The excitation wavelength used was 358 nm and emission was monitored at 430 nm. Fluorescence anisotropy measurements were carried out with membranes containing 100 nmol phospholipid at a probe to phospholipid ratio of 1:100 (mol/mol) at room temperature (~23 °C). Data represent means ± S.E. from at least three independent experiments. The line joining the data points is provided merely as a viewing guide. The chemical structure of DPH is shown in the inset. See Section 2 for more details.

Table 1
Membrane concentrations of PEtOH from total concentrations derived using membrane/buffer partition coefficient.[a]

Total concentration (C_T) % (v/v)	Membrane concentration (C_M) % (v/v)
0.01	0.008
0.03	0.025
0.05	0.041
0.08	0.066
0.10	0.082
0.25	0.205
0.50	0.410

[a] Membrane/buffer partition coefficient of PEtOH (4.58) was taken from McCreery and Hunt (1978).

3.2. Inhibition of specific radioligand binding to the serotonin$_{1A}$ receptor in the presence of PEtOH

The popularity of serotonin$_{1A}$ receptors among the serotonin receptor family members stems from the early availibility of selective agonist (8-OH-DPAT) and antagonist (*p*-MPPF) that allows widespread biochemical, physiological, and pharmacological characterization of the receptor (Gozlan et al., 1983; Kung et al., 1996). Fig. 1 shows the effect of increasing concentrations of PEtOH on binding of the specific agonist [^{3}H]8-OH-DPAT, and antagonist [^{3}H]*p*-MPPF, to serotonin$_{1A}$ receptors in hippocampal membranes. As evident from the figure, there is a decrease in specific binding of both agonist and antagonist to the receptor in the presence of PEtOH, in a concentration-dependent manner. The extent of reduction in specific binding over the range of PEtOH concentration used for the agonist and antagonist was similar (>90%), although the reduction in specific binding is more gradual in case of the antagonist. The figure shows 50% inhibition in specific binding at concentrations of 0.016% (agonist) and 0.114% (antagonist) (v/v). The presence of PEtOH therefore inhibited specific ligand binding to the serotonin$_{1A}$ receptor.

3.3. Altered binding affinity of [^{3}H]8-OH-DPAT to the serotonin$_{1A}$ receptor in PEtOH-treated hippocampal membranes

In order to address the change in specific agonist binding, we measured the binding affinity of the specific agonist [^{3}H]8-OH-DPAT to the serotonin$_{1A}$ receptor in the presence of PEtOH. Saturation binding analysis for binding of the specific agonist [^{3}H]8-OH-DPAT to the serotonin$_{1A}$ receptor is shown in Fig. 2 and corresponding binding parameters obtained upon fitting the curves are shown in Table 2. The results obtained from saturation binding analysis in control and PEtOH-treated membranes indicate that the decrease in ligand binding resulted due to decreased affinity of the agonist for the receptor, as the number of maximum binding sites was found to be comparable in both cases. There was a significant increase in K_d (~3 fold higher, $p < 0.001$) in case of PEtOH-treated hippocampal membranes with respect to native membranes, whereas the change in B_{max} was found to be not significant. This implies that the binding affinity of [^{3}H]8-OH-DPAT to serotonin$_{1A}$ receptors is reduced in the presence of PEtOH.

3.4. G-protein coupling efficiency of the receptor is decreased in the presence of PEtOH

To assess whether PEtOH could affect signaling mediated by serotonin$_{1A}$ receptors, we carried out GTP-γ-S sensitivity assay which provides information on receptor/G-protein coupling (Harikumar and Chattopadhyay, 1999). G-proteins negatively couple the serotonin$_{1A}$ receptor to the adenylate cyclase system (Harikumar and Chattopadhyay, 1999; Emerit et al., 1990). Agonist binding to GPCRs exhibits sensitivity to GTP-γ-S, a non-hydrolyzable (strictly speaking, a very slowly hydrolyzable analogue (Eccleston et al., 2002)) of GTP, which uncouples the regular cycle of guanine nucleotide exchange at the G_α subunit upon activation of the receptor. We have previously reported that GTP-γ-S promotes a transition of the hippocampal serotonin$_{1A}$ receptor from a high-affinity G-protein-coupled state to a low-affinity G-protein-uncoupled state (Harikumar and Chattopadhyay, 1999). There is a reduction in specific binding of the agonist [^{3}H]8-OH-DPAT with increasing concentrations of GTP-γ-S (see Fig. 3) with a half-maximal inhibition concentration (IC_{50}) of 102.2 nM for native hippocampal membranes (see Table 3). The inhibition curve of PEtOH-treated hippocampal membranes exhibited a significant ($p < 0.05$) shift toward higher concentrations of GTP-γ-S with a higher IC_{50} value of 189.7 nM (see Table 3). These results imply that agonist binding to the serotonin$_{1A}$ receptor upon PEtOH treatment is less sensitive to GTP-γ-S, pointing out the effect on G-protein coupling efficiency under these conditions. This indicates that G-protein coupling of the receptor is decreased in the presence of PEtOH. Membrane lipids have been reported to play a role in the interaction of G-proteins with the membrane, which could modulate their interaction with the receptors (Escribá et al., 1995, 1997; Inagaki et al., 2012; Dawaliby et al., 2015; Vögler et al., 2004). It is possible that the presence of PEtOH affects the interaction of G-proteins with membrane lipids, which could affect the G-protein coupling mediated by the serotonin$_{1A}$ receptor.

3.5. Fluorescence anisotropy of DPH in PEtOH-treated hippocampal membranes

Local anesthetics may act through specific localized interactions with GPCRs or through more global (general) lipid-mediated effects. To probe whether PEtOH in general alters membrane order, we measured fluorescence anisotropy of DPH in native and PEtOH-treated hippocampal membranes. DPH has a rod-like shape and partitions into the interior of membrane bilayers (Lentz, 1989). Fluorescence anisotropy of membrane embedded probes such as DPH is commonly used to monitor the rate of rotational diffusion, as reorientation of the fluorophore is dependent on packing of acyl chains in membrane bilayers (Lakowicz, 2006; Jameson and Ross, 2010). An advantage of using DPH in studies with natural membranes like the hippocampal membrane is that its distribution in the membrane is independent of membrane phase (London and Feigenson, 1981). Fig. 4 shows that the fluorescence anisotropy of DPH shows progressive reduction with increase in PEtOH concentration. The value of DPH anisotropy (~0.23) in native hippocampal membranes (in the absence of PEtOH) suggests liquid-ordered nature of hippocampal membranes. In the liquid-ordered phase, acyl chains are elongated and ordered (as seen in the gel or ordered phase), but exhibit high translational mobility similar to the liquid-disordered phase (Mouritsen, 2010). The liquid-ordered nature of hippocampal membranes has also been supported by wavelength-dependence of Laurdan generalized polarization (GP) (Mukherjee and Chattopadhyay, 2005), and order parameters from electron spin resonance (ESR) spectra of spin-labeled phospholipids (Singh et al., 2012). The liquid-ordered nature of hippocampal membranes could be attributed to high content of cholesterol (>30 mol%) (Pucadyil and Chattopadhyay,

Table 2
Effect of PEtOH on specific [^{3}H]8-OH-DPAT binding parameters to serotonin$_{1A}$ receptors.[a]

Condition	K_d (nM)	B_{max} (fmol/mg of protein)
Native membrane	0.87 ± 0.13	74.6 ± 8.3
PEtOH-treated membrane	3.48 ± 0.22[b]	70.1 ± 3.6[b]

[a] The binding parameters shown represent means ± S.E. from three independent experiments, while saturation binding data shown in Fig. 2 is from a representative experiment. PEtOH concentration was 0.04% (v/v). See Section 2 for more details.
[b] A significant increase in K_d ($p < 0.001$) was observed, whereas the change in B_{max} was found to be not significant.

Table 3
Effect of PEtOH on the efficiency of G-protein coupling to serotonin$_{1A}$ receptors.[a]

Condition	IC_{50} (nM)
Native membrane	102.2 ± 20.7
PEtOH-treated membrane	189.7 ± 6.1[b]

[a] The binding parameters shown represent means ± S.E. from three independent experiments. PEtOH concentration was 0.04% (v/v). See Section 2 for more details.
[b] The increase in the IC_{50} value was found to be significant ($p < 0.05$).

2004b). We have recently shown that PEtOH causes disorder in membranes depending on the specific phase of the membrane (Shrivastava et al., 2016). The disordering observed in liquid-ordered membranes was found to be between gel and fluid phases. Fig. 4 shows that fluorescence anisotropy of DPH was reduced by ~12% at the highest concentration of PEtOH used. This indicates that membrane packing is altered in PEtOH-treated membranes and the lipid acyl chains could be more disordered in presence of PEtOH. Such reduction in membrane order by PEtOH could contribute to change in receptor activity.

3.6. Fluorescence lifetime and apparent rotational correlation time of DPH in PEtOH-treated hippocampal membranes

Fluorescence lifetime is a reliable indicator of polarity changes in the immediate surrounding environment of a fluorophore (Prendergast, 1991). We wanted to explore changes in membrane environment in the presence of PEtOH by fluorescence lifetime measurements of DPH. The fluorescence lifetime of DPH is known to be responsive to polarity changes in its surroundings (Stubbs et al., 1995; Shrivastava et al., 2008). The fluorescence decays obtained could be fitted well to a biexponential function. Intensity-averaged mean fluorescence lifetimes were calculated since it does not depend on the method of analysis and the number of exponentials used to fit the time-resolved fluorescence decay. The lifetimes of DPH in native and PEtOH-treated hippocampal membranes are shown in Table 4. The mean fluorescence lifetimes of DPH under these conditions were calculated from data shown in Table 4 using Eq. (5), and are displayed in Fig. 5a. We observed a modest reduction in fluorescence lifetime of DPH with increasing concentration of PEtOH, amounting to ~4% decrease in lifetime with the highest concentration of PEtOH.

In order to ensure that DPH anisotropy values (Fig. 4) measured were not influenced by lifetime-induced artifacts, we calculated the apparent rotational correlation time (see Fig. 5b), as described earlier (Saxena et al., 2015), using r_o value of 0.36 (Shinitzky and Barenholz, 1974). With increasing PEtOH concentration, the change in apparent rotational correlation time displayed a similar trend, as observed with anisotropy change with increasing PEtOH (Fig. 4) concentration, although the magnitude of the change was large (~30%; see Fig. 5b).

3.7. Correlation between apparent rotational correlation time and specific binding of the agonist

In order to obtain an insight into membrane property changes induced by PEtOH and receptor function (activity), we generated a plot of the specific agonist binding to the serotonin$_{1A}$ receptor (taken from Fig. 1) as a function of apparent rotational correlation time (from Fig. 5b), with increasing concentration of PEtOH. The concentration of PEtOH used in each case is also shown in the upper axis. The resultant plot is shown in Fig. 6. The plot exhibited little change in rotational correlation time, but large change in receptor activity at lower concentrations of PEtOH, followed by a linear decrease in both parameters at higher concentrations of PEtOH. This implies that PEtOH-induced modulation of receptor activity could depend on membrane order at high anesthetic concentration. Interestingly, at lower anesthetic concentration, this behavior changes and receptor activity appears to be independent of membrane order. We interpret this as receptor activity being modulated by a combined mechanism of general (global) membrane effect (*i.e.*, membrane order) and specific (direct) effect in the presence of PEtOH. Interestingly, a non-linear regression analysis between apparent rotational correlation and specific agonist binding time gave a correlation coefficient of (r) ~0.98. All data points were present within the 90% confidence intervals, highlighting that the tight correlation between these two parameters is significant.

Table 4
Representative fluorescence lifetimes of DPH in hippocampal membranes with increasing concentrations of PEtOH.[a]

% PEtOH (v/v)	α_1	τ_1 (ns)	α_2	τ_2 (ns)
0	0.23	0.06	0.77	10.87
0.01	0.24	0.07	0.76	10.80
0.03	0.18	0.07	0.82	10.86
0.05	0.27	0.05	0.73	10.87
0.08	0.18	0.06	0.82	10.81
0.10	0.17	0.08	0.83	10.84
0.25	0.11	0.10	0.89	10.68
0.50	0.12	0.11	0.88	10.42

[a] The excitation wavelength was 374 nm and emission was monitored at 430 nm in all cases. The ratio of DPH to total lipid was 1:100 (mol/mol). See Section 2 for more details.

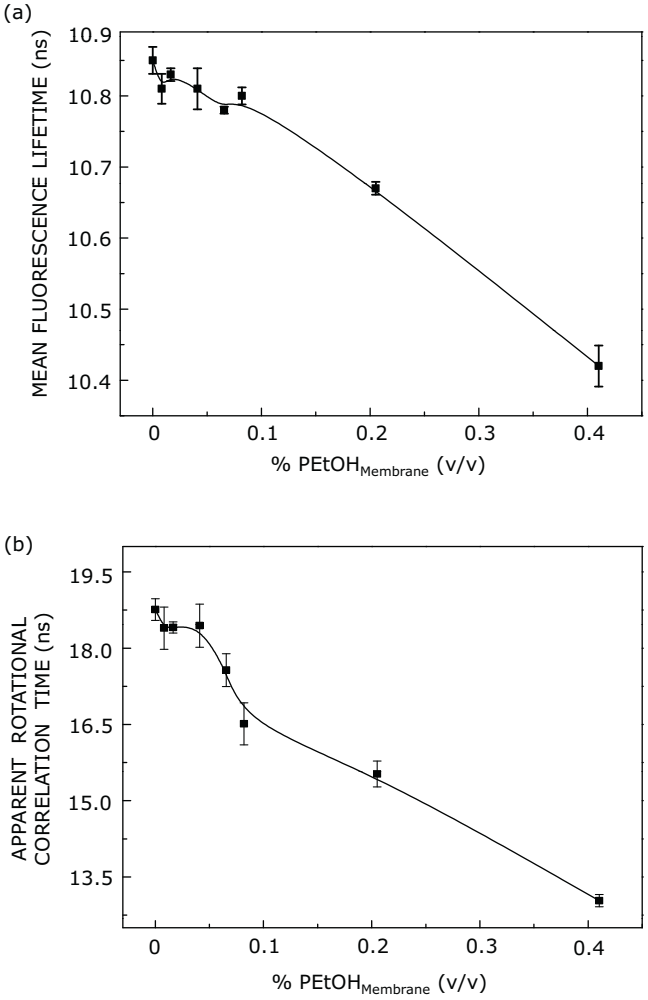

Fig. 5. (a) Mean fluorescence lifetimes of DPH in hippocampal membranes with increasing concentrations of PEtOH. Mean fluorescence lifetimes were calculated using Eq. (5). The excitation wavelength used was 374 nm and emission was monitored at 430 nm. Data shown are means ± S.E. of at least three independent measurements. All other conditions are as in Fig. 4. See Section 2 and Table 4 for more details. (b) Apparent rotational correlation times of DPH in hippocampal membranes with increasing concentrations of PEtOH. Apparent rotational correlation times were calculated from fluorescence anisotropy values from Fig. 4 and mean fluorescence lifetimes from Fig. 5a. Lines joining data points are provided merely as viewing guides. The PEtOH concentration plotted in both panels is the actual concentration of PEtOH partitioned into the membrane. See text for more details.

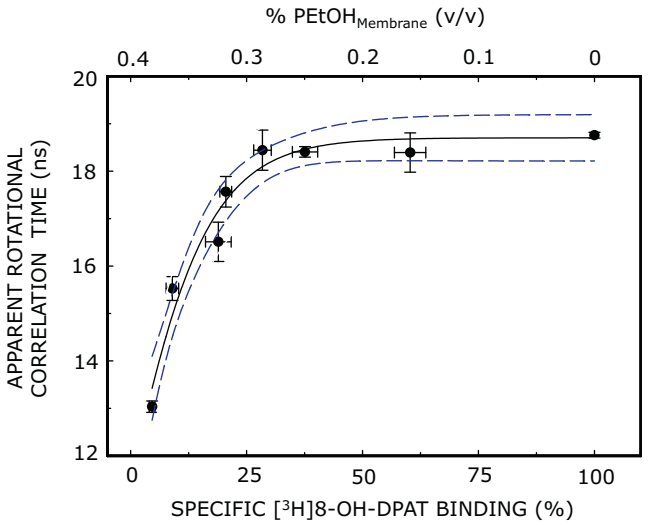

Fig. 6. Correlation of specific binding of [^{3}H]8-OH-DPAT to the serotonin$_{1A}$ receptor with apparent rotational correlation time of DPH in hippocampal membranes with increasing concentrations of PEtOH. Specific [^{3}H]8-OH-DPAT binding to the serotonin$_{1A}$ receptor (values taken from Fig. 1) and corresponding values of apparent rotational correlation time of DPH (from Fig. 5b) are plotted. Non-linear regression analysis yielded a correlation coefficient (r) ~0.98. The significance of the correlation is apparent from the 90% confidence interval (plotted as dashed lines). See text for more details.

4. Discussion

The effects of anesthetics on GPCRs constitute an emerging area of research (Minami and Uezono, 2013). This is because the exact mechanism underlying anesthetics action remains elusive. In this study, we have examined the effect of PEtOH, a local anesthetic, on the function of the hippocampal serotonin$_{1A}$ receptor, an important neurotransmitter receptor, which belongs to the GPCR superfamily. The hippocampal membrane serves as an excellent source for the serotonin$_{1A}$ receptor. We have previously established bovine hippocampal membranes as a convenient source to study the interaction of membrane lipids with neuronal GPCRs such as the serotonin$_{1A}$ receptor (Pucadyil and Chattopadhyay, 2004a). The rich and diverse lipid composition of the nervous system (Bozek et al., 2015; Sastry, 1985) provides a comprehensive functional backdrop for efficient functioning of neuronal receptors.

Our results show that PEtOH induces reduction in agonist binding to the serotonin$_{1A}$ receptor due to lowering of binding affinity. In addition, a concomitant decrease in the level of G-protein coupling is observed. Analysis of membrane environment using the environment-sensitive fluorescent probe DPH revealed decrease in membrane order, as apparent from reduction in rotational correlation time, with increasing PEtOH concentration. Interestingly, the changes in ligand binding and membrane order exhibited tight correlation up to a certain threshold ligand occupancy (receptor activity ~30%). These results are reminiscent of our previous observations that agonist binding of the hippocampal serotonin$_{1A}$ receptor was decreased in the presence of capsaicin, which alters membrane physical properties by enhancing the membrane elasticity (Prasad et al., 2009). In addition, these results agree with our recent findings of a direct correlation between membrane viscosity (monitored using a fluorescent molecular rotor) and receptor activity (Pal et al., 2016), suggesting the important role of membrane physical properties in receptor function. On the other hand, beyond the threshold occupancy (~30%), a large change in specific agonist binding was observed, without appreciable change in membrane order, as reported by apparent rotational correlation time of DPH. This points out to a lack of dependence of receptor activity on membrane order in this occupancy regime, possibly due to specific interaction taking over as the major determinant of receptor-ligand interaction. Although it is tempting to speculate the molecular basis for such a switch in the mechanism controlling receptor-ligand interaction, it is not obvious from our data. We plan to set up detailed molecular dynamics simulations to address this further to arrive at a comprehensive model for such duality in receptor-ligand interaction.

Membrane order has physiological implications in GPCR function (Escribá et al., 2007). Several diseases where GPCR signaling plays an essential role, such as hypertension and Alzheimer's disease, are characterized by change in membrane order (Roth et al., 1995; Zicha et al., 1999). On the other hand, the role of specific effects on receptor function has been aptly shown from our previous work on the effect of membrane cholesterol on serotonin$_{1A}$ receptor function. Earlier work from our laboratory has comprehensively established the need of membrane cholesterol in serotonin$_{1A}$ receptor function (reviewed in (Jafurulla and Chattopadhyay, 2013; Paila et al., 2010; Pucadyil et al., 2005; Pucadyil and Chattopadhyay, 2006)). A large body of work has shown that the interaction between membrane cholesterol and the serotonin$_{1A}$ receptor appears to be structurally stringent, as immediate biosynthetic precursors of cholesterol (differing with cholesterol in just a double bond) were unable to preserve receptor function (Paila et al., 2008; Singh et al., 2009). In further support of this view, we previously showed that cholesterol requirement for serotonin$_{1A}$ receptor function is diastereospecific, yet not enantiospecific (Jafurulla et al., 2014). In addition, we showed that this differential sterol stereospecificity for receptor function could be related to membrane dipole potential (Bandari et al., 2014). In a parallel work, we demonstrated using coarse-grain molecular dynamics simulations, that membrane cholesterol has higher occupancy in certain sites on the serotonin$_{1A}$ receptor (Sengupta and Chattopadhyay, 2012). Overall, these results appear to support a specific mechanism for receptor-ligand interaction in the membrane. It must therefore be stated here that the role of specific and general effects in the function of membrane proteins and receptors continues to evolve (Lee, 2011; Paila and Chattopadhyay, 2009). Moreover, as shown here, the above mechanisms may not be mutually exclusive, and could operate simultaneously, fine-tuned by a switch such as receptor occupancy levels.

In summary, we show here that the local anesthetic PEtOH affects ligand binding properties and G-protein coupling to the hippocampal serotonin$_{1A}$ receptor. Further, we show that the change in receptor activity is due to a combination of alteration in membrane order induced by PEtOH and specific receptor-ligand interaction in the presence of PEtOH. These results demonstrate that local anesthetics influence GPCR function and this could have implications on various physiological processes occuring during anesthesia. We envisage that the action of local anesthetics could involve a combination of specific interaction of the receptor with anesthetics and modulation of properties of the membrane lipid environment.

Conflict of interest

The authors declare that there is no conflict of interest.

Acknowledgments

This work was supported by the Council of Scientific and Industrial Research (Govt. of India) Network project MIND (BSC0115). B.D.R. thanks the University Grants Commission for the award of a Senior Research Fellowship. A.C. is an Adjunct Professor of Tata Institute of Fundamental Research (Mumbai),

RMIT University (Melbourne, Australia), Indian Institute of Technology (Kanpur), and Indian Institute of Science Education and Research (Mohali). A.C. gratefully acknowledges J.C. Bose Fellowship (Department of Science and Technology, Govt. of India). We thank Md. Jafurulla, Parijat Sarkar, and G. Aditya Kumar for help with experiments and useful discussion, and members of the Chattopadhyay laboratory for critically reading the manuscript.

References

Anbazhagan, V., Munz, C., Tome, L., Schneider, D., 2010. Fluidizing the membrane by a local anesthetic: phenylethanol affects membrane protein oligomerization. J. Mol. Biol. 404, 773–777.
Arias, H.R., 1999. Role of local anesthetics on both cholinergic and serotonergic ionotropic receptors. Neurosci. Biobehav. Rev. 23, 817–843.
Bandari, S., Chakraborty, H., Covey, D.F., Chattopadhyay, A., 2014. Membrane dipole potential is sensitive to cholesterol stereospecificity: implications for receptor function. Chem. Phys. Lipids 184, 25–29.
Bozek, K., Wei, Y., Yan, Z., Liu, X., Xiong, J., Sugimoto, M., Tomita, M., Pääbo, S., Sherwood, C.C., Hof, P.R., Ely, J.J., Li, Y., Steinhauser, D., Willmitzer, L., Giavalisco, P., Khaitovich, P., 2015. Organization and evolution of brain lipidome revealed by large-scale analysis of human, chimpanzee, macaque, and mouse tissues. Neuron 85, 695–702.
Bruns, R.F., Lawson-Wendling, K., Pugsley, T.A., 1983. A rapid filtration assay for soluble receptors using polyethylenimine-treated filters. Anal. Biochem. 132, 74–81.
Cantor, R.S., 2001. Breaking the Meyer-Overton rule: predicted effects of varying stiffness and interfacial activity on the intrinsic potency of anesthetics. Biophys. J. 80, 2284–2297.
Chanda, P.K., Minchin, M.C.W., Davis, A.R., Greenberg, L., Reilly, Y., McGregor, W.H., Bhat, R., Lubeck, M.D., Mizutani, S., Hung, P.P., 1993. Identification of residues important for ligand binding to the human 5-hydroxytryptamine$_{1A}$ serotonin receptor. Mol. Pharmacol. 43, 516–520.
Chattopadhyay, A., London, E., 1984. Fluorimetric determination of critical micelle concentration avoiding interference from detergent charge. Anal. Biochem. 139, 408–412.
Chattopadhyay, A., 2014. GPCRs: lipid-dependent membrane receptors that act as drug targets. Adv. Biol. 2014, 143023.
Corre, J., Lucchini, J.J., Mercier, G.M., Cremieux, A., 1990. Antibacterial activity of phenethyl alcohol and resulting membrane alterations. Res. Microbiol. 141, 483–497.
Dawaliby, R., Trubbia, C., Delporte, C., Masureel, M., Van Antwerpen, P., Kobilka, B.K., Govaerts, C., 2015. Allosteric regulation of G protein–coupled receptor activity by phospholipids. Nat. Chem. Biol. 12, 35–41.
Eccleston, J.F., Binns, D.D., Davis, C.T., Albanesi, J.P., Jameson, D.M., 2002. Oligomerization and kinetic mechanism of the dynamin GTPase. Eur. Biophys. J. 31, 275–282.
Emerit, M.B., El Mestikawy, S., Gozlan, H., Rouot, B., Hamon, M., 1990. Physical evidence of the coupling of solubilized 5-HT$_{1A}$ binding sites with G regulatory proteins. Biochem. Pharmacol. 39, 7–18.
Escribá, P.V., Sastre, M., García-Sevilla, J.A., 1995. Disruption of cellular signaling pathways by daunomycin through destabilization of nonlamellar membrane structures. Proc. Natl. Acad. Sci. U. S. A. 92, 7595–7599.
Escribá, P.V., Ozaita, A., Ribas, C., Miralles, A., Fodor, E., Farkas, T., García-Sevilla, J.A., 1997. Role of lipid polymorphism in G protein-membrane interactions: nonlamellar-prone phospholipids and peripheral protein binding. Proc. Natl. Acad. Sci. U. S. A. 94, 11375–11380.
Escribá, P.V., Wedegaertner, P.B., Goñi, F.M., Vögler, O., 2007. Lipid-protein interactions in GPCR-associated signaling. Biochim. Biophys. Acta 1768, 836–852.
Fiorino, F., Severino, B., Magli, E., Ciano, A., Caliendo, G., Santagada, V., Frecentese, F., Perissutti, E., 2014. 5-HT$_{1A}$ receptor: an old target as a new attractive tool in drug discovery from central nervous system to cancer. J. Med. Chem. 57, 4407–4426.
Fozzard, H.A., Lee, P.J., Lipkind, G.M., 2005. Mechanism of local anesthetic drug action on voltage-gated sodium channels. Curr. Pharm. Des. 11, 2671–2686.
Franks, N.P., Lieb, W.R., 1997. Inhibitory synapses: anaesthetics set their sites on ion channels. Nature 389, 334–335.
Fredriksson, R., Lagerström, M.C., Lundin, L.-G., Schiöth, H.B., 2003. The G-protein-coupled receptors in the human genome form five main families. Phylogenetic analysis, paralogon groups, and fingerprints. Mol. Pharmacol. 63, 1256–1272.
Gozlan, H., El Mestikawy, S., Pichat, L., Glowinski, J., Hamon, M., 1983. Identification of presynaptic serotonin autoreceptors using a new ligand: ^{3}H-PAT. Nature 305, 140–142.
Gray, E., Karslake, J., Machta, B.B., Veatch, S.L., 2013. Liquid general anesthetics lower critical temperatures in plasma membrane vesicles. Biophys. J. 105, 2751–2759.
Grinvald, A., Steinberg, I.Z., 1974. On the analysis of fluorescence decay kinetics by the method of least-squares. Anal. Biochem. 59, 583–598.
Harikumar, K.G., Chattopadhyay, A., 1999. Differential discrimination of G-protein coupling of serotonin$_{1A}$ receptors from bovine hippocampus by an agonist and an antagonist. FEBS Lett. 457, 389–392.
Higashijima, T., Ferguson, K.M., Sternweis, P.C., Smigel, M.D., Gilman, A.G., 1987. Effects of Mg^{2+} and the $\beta\gamma$-subunit complex on the interactions of guanine nucleotides with G proteins. J. Biol. Chem. 262, 762–766.
Ho, B.Y., Karschin, A., Branchek, T., Davidson, N., Lester, H.A., 1992. The role of conserved aspartate and serine residues in ligand binding and in function of the 5-HT$_{1A}$ receptor: a site directed mutation study. FEBS Lett. 312, 259–262.
Hollmann, M.W., Strumper, S., Herroeder, S., Durieux, M.E., 2005. Receptors, G proteins, and their interactions. Anesthesiology 103, 1066–1078.
Inagaki, S., Ghirlando, R., White, J.F., Gvozdenovic-Jeremic, J., Northup, J.K., Grisshammer, R., 2012. Modulation of the interaction between neurotensin receptor NTS1 and Gq protein by lipid. J. Mol. Biol. 417, 95–111.
Ishizawa, Y., Pidikiti, R., Liebman, P.A., Eckenhoff, R.G., 2002. G protein-coupled receptors as direct targets of inhaled anesthetics. Mol. Pharmacol. 61, 945–952.
Jacobson, K.A., 2015. New paradigms in GPCR drug discovery. Biochem. Pharmacol. 98, 541–555.
Jafurulla, M., Chattopadhyay, A., 2013. Membrane lipids in the function of serotonin and adrenergic receptors. Curr. Med. Chem. 20, 47–55.
Jafurulla, M., Rao, B.D., Sreedevi, S., Ruysschaert, J.-M., Chattopadhyay, A., 2014. Stereospecific requirement of cholesterol in the function of the serotonin$_{1A}$ receptor. Biochim. Biophys. Acta 1838, 158–163.
Jameson, D.M., Ross, J.A., 2010. Fluorescence polarization/anisotropy in diagnostics and imaging. Chem. Rev. 110, 2685–2708.
Jordi, W., Nibbeling, R., de Kruijff, B., 1990. Phenethyl alcohol disorders phospholipid acyl chains and promotes translocation of the mitochondrial precursor protein apocytochrome *c* across a lipid bilayer. FEBS Lett. 261, 55–58.
Kalipatnapu, S., Chattopadhyay, A., 2004. Interaction of serotonin$_{1A}$ receptors from bovine hippocampus with tertiary amine local anesthetics. Cell. Mol. Neurobiol. 24, 403–422.
Killian, J.A., Fabrie, C.H.J.P., Baart, W., Morein, S., de Kruijff, B., 1992. Effects of temperature variation and phenethyl alcohol addition on acyl chain order and lipid organization in *Escherichia coli* derived membrane systems A ^{2}H- and ^{31}P-NMR study. Biochim. Biophys. Acta 1105, 253–262.
Kung, H.F., Stevenson, Z.-P., Zhuang, M.-P., Kung, M.-P., Frederick, D., Hurt, S.D., 1996. New 5-HT$_{1A}$ receptor antagonist: [^{3}H]*p*-MPPF. Synapse 23, 344–346.
Lakowicz, J.R., 2006. Principles of Fluorescence Spectroscopy, 3rd ed. Springer, New York.
Lampert, R.A., Chewter, L.A., Phillips, D., O'Connor, D.V., Roberts, A.J., Meech, S.R., 1983. Standards for nanosecond fluorescence decay time measurements. Anal. Chem. 55, 68–73.
Lee, A.G., 2011. Biological membranes: the importance of molecular detail. Trends Biochem. Sci. 36, 493–500.
Lentz, B.R., 1989. Membrane fluidity as detected by diphenylhexatriene probes. Chem. Phys. Lipids 50, 171–190.
London, E., Feigenson, G.W., 1981. Fluorescence quenching in model membranes: an analysis of the local phospholipid environments of diphenylhexatriene and gramicidin A'. Biochim. Biophys. Acta 649, 89–97.
Matsunaga, F., Gao, L., Huang, X.-P., Saven, J.G., Roth, B.L., Liu, R., 2015. Molecular interactions between general anesthetics and the 5HT$_{2B}$ receptor. J. Biomol. Struct. Dyn. 33, 211–218.
McClare, C.W.F., 1971. An accurate and convenient organic phosphorus assay. Anal. Biochem. 39, 527–530.
McCreery, M.J., Hunt, W.A., 1978. Physico-chemical correlates of alcohol intoxication. Neuropharmacology 17, 451–461.
Minami, K., Uezono, Y., 2013. The recent progress in research on effects of anesthetics and analgesics on G protein-coupled receptors. J. Anesth. 27, 284–292.
Mouritsen, O.G., 2010. The liquid-ordered state comes of age. Biochim. Biophys. Acta 1798, 1286–1288.
Mukherjee, S., Chattopadhyay, A., 2005. Monitoring the organization and dynamics of bovine hippocampal membranes utilizing laurdan generalized polarization. Biochim. Biophys. Acta 1714, 43–55.
Nakayama, T., Hayashi, M., Warner, D.O., Jones, K.A., 2005. Anesthetics inhibit membrane receptor coupling to the $G_{q/11}$ heterotrimeric G protein in airway smooth muscle. Anesthesiology 103, 296–305.
Nichols, D.E., Nichols, C.D., 2008. Serotonin receptors. Chem. Rev. 108, 1614–1641.
Paila, Y.D., Chattopadhyay, A., 2009. The function of G-protein coupled receptors and membrane cholesterol: specific or general interaction? Glycoconj. J. 26, 711–720.
Paila, Y.D., Murty, M.R.V.S., Vairamani, M., Chattopadhyay, A., 2008. Signaling by the human serotonin$_{1A}$ receptor is impaired in cellular model of Smith-Lemli-Opitz syndrome. Biochim. Biophys. Acta 1778, 1508–1516.
Paila, Y.D., Dutta, A., Chattopadhyay, A., 2010. Membrane cholesterol in the function and organization of G-protein coupled receptors. Subcell. Biochem. 51, 439–466.
Paila, Y.D., Tiwari, S., Sengupta, D., Chattopadhyay, A., 2011. Molecular modeling of the human serotonin$_{1A}$ receptor: role of membrane cholesterol in ligand binding of the receptor. Mol. Biosyst. 7, 224–234.
Pal, S., Chakraborty, H., Bandari, S., Yahioglu, G., Suhling, K., Chattopadhyay, A., 2016. Molecular rheology of neuronal membranes explored using a molecular rotor: implications for receptor function. Chem. Phys. Lipids 196, 69–75.
Peterlin, Z., Ishizawa, Y., Areneda, R., Eckenhoff, R., Firestein, S., 2005. Selective activation of G-protein coupled receptors by volatile anesthetics. Mol. Cell. Neurosci. 30, 506–512.
Picardi, S., Stevens, M.F., Hahnenkamp, K., Durieux, M.E., Lirk, P., Hollmann, M.W., 2014. Time-dependent modulation of muscarinic m1/m3 receptor signalling by local anaesthetics. Br. J. Anaesth. 112, 370–379.
Pierce, K.L., Premont, R.T., Lefkowitz, R.J., 2002. Seven-transmembrane receptors. Nat. Rev. Mol. Cell Biol. 3, 639–650.

Prasad, R., Singh, P., Chattopadhyay, A., 2009. Effect of capsaicin on ligand binding activity of the hippocampal serotonin$_{1A}$ receptor. Glycoconj. J. 26, 733–738.
Prendergast, F.G., 1991. Time-resolved fluorescence techniques: methods and applications in biology. Curr. Opin. Struct. Biol. 1, 1054–1059.
Pucadyil, T.J., Chattopadhyay, A., 2004a. Cholesterol modulates ligand binding and G-protein coupling to serotonin$_{1A}$ receptors from bovine hippocampus. Biochim. Biophys. Acta 1663, 188–200.
Pucadyil, T.J., Chattopadhyay, A., 2004b. Exploring detergent insolubility in bovine hippocampal membranes: a critical assessment of the requirement for cholesterol. Biochim. Biophys. Acta 1661, 9–17.
Pucadyil, T.J., Chattopadhyay, A., 2006. Role of cholesterol in the function and organization of G-protein coupled receptors. Prog. Lipid Res. 45, 295–333.
Pucadyil, T.J., Kalipatnapu, S., Chattopadhyay, A., 2005. The serotonin$_{1A}$ receptor: a representative member of the serotonin receptor family. Cell. Mol. Neurobiol. 25, 553–580.
Rehberg, B., Urban, B.W., Duch, D.S., 1995. The membrane lipid cholesterol modulates anesthetic actions on a human brain ion channel. Anesthesiology 82, 749–758.
Rosenbaum, D.M., Rasmussen, S.G.F., Kobilka, B.K., 2009. The structure and function of G-protein-coupled receptors. Nature 459, 356–363.
Roth, G.S., Joseph, J.A., Mason, R.P., 1995. Membrane alterations as causes of impaired signal transduction in Alzheimer's disease and aging. Trends Neurosci. 18, 203–206.
Sastry, P.S., 1985. Lipids of nervous tissue: composition and metabolism. Prog. Lipid Res. 24, 69–176.
Saxena, R., Shrivastava, S., Chattopadhyay, A., 2015. Cholesterol-induced changes in hippocampal membranes utilizing a phase-sensitive fluorescence probe. Biochim. Biophys. Acta 1848, 1699–1705.
Sengupta, D., Chattopadhyay, A., 2012. Identification of cholesterol binding sites in the serotonin$_{1A}$ receptor. J. Phys. Chem. B 116, 12991–12996.
Shinitzky, M., Barenholz, Y., 1974. Dynamics of the hydrocarbon layer in liposomes of lecithin and sphingomyelin containing dicetylphosphate. J. Biol. Chem. 249, 2652–2657.
Shrivastava, S., Paila, Y.D., Dutta, A., Chattopadhyay, A., 2008. Differential effects of cholesterol and its immediate biosynthetic precursors on membrane organization. Biochemistry 47, 5668–5677.
Shrivastava, S., Dutta, D., Chattopadhyay, A., 2016. Effect of local anesthetics on the organization and dynamics in membranes of varying phase: a fluorescence approach. Chem. Phys. Lipids 198, 21–27.
Singh, P., Saxena, R., Paila, Y.D., Jafurulla, M., Chattopadhyay, A., 2009. Differential effects of cholesterol and desmosterol on the ligand binding function of the hippocampal serotonin$_{1A}$ receptor: implications in desmosterolosis. Biochim. Biophys. Acta 1788, 2169–2173.
Singh, P., Tarafdar, P.K., Swamy, M.J., Chattopadhyay, A., 2012. Organization and dynamics of hippocampal membranes in a depth-dependent manner: an electron spin resonance study. J. Phys. Chem. B 116, 2999–3006.
Smith, P.K., Krohn, R.I., Hermanson, G.T., Mallia, A.K., Gartner, F.H., Provenzano, M.D., Fujimoto, E.K., Goeke, N.M., Olson, B.J., Klenk, D.C., 1985. Measurement of protein using bicinchoninic acid. Anal. Biochem. 150, 76–85.
Stubbs, C.D., Ho, C., Slater, S.J., 1995. Fluorescence techniques for probing water penetration into lipid bilayers. J. Fluoresc. 5, 19–28.
Tautermann, C.S., 2014. GPCR structures in drug design, emerging opportunities with new structures. Bioorg. Med. Chem. Lett. 24, 4073–4079.
Vögler, O., Casas, J., Capó, D., Nagy, T., Borchert, G., Martorell, G., Escribá, P.V., 2004. The G$\beta\gamma$ dimer drives the interaction of heterotrimeric G$_i$ proteins with nonlamellar membrane structures. J. Biol. Chem. 279, 36540–36545.
Zhang, Y., DeVries, M.E., Skolnick, J., 2006. Structure modeling of all identified G protein-coupled receptors in the human genome. PLoS Comput. Biol. 2, e13.
Zicha, J., Kunes, J., Devynck, M.-A., 1999. Abnormalities of membrane function and lipid metabolism in hypertension: a review. Am. J. Hypertens. 12, 315–331.